IEEE Access
Multidisciplinary | Rapid Review | Open Access Journal

Received December 10, 2020, accepted January 12, 2021, date of publication January 25, 2021, date of current version February 4, 2021.

Digital Object Identifier 10.1109/ACCESS.2021.3054600

PI-Type Controllers and Σ−Δ Modulation for Saturated DC-DC Buck Power Converters

CARLOS AGUILAR-IBANEZ[1], JAVIER MORENO-VALENZUELA[2], (Member, IEEE), O. GARCÍA-ALARCÓN[3], MIZRAIM MARTINEZ-LOPEZ[2], JOSÉ ÁNGEL ACOSTA[4], AND MIGUEL S. SUAREZ-CASTANON[5]

[1]Instituto Politécnico Nacional-CIC, Ciudad de México 07738, México
[2]Instituto Politécnico Nacional-CITEDI, Tijuana 22435, México
[3]Tecnológico Nacional de México-Instituto Tecnológico Superior de Cosamaloapan, Veracruz 95400, México
[4]Departamento de Ingeniería de Sistemas y Automática, Escuela Técnica Superior de Ingeniería, Camino de los Descubrimientos s.n., Universidad de Sevilla, 41092 Seville, Spain
[5]Instituto Politécnico Nacional-ESCOM, Ciudad de México 07738, México

Corresponding author: Javier Moreno-Valenzuela (moreno@citedi.mx)

This work was supported in part by the Instituto Politécnico Nacional under Grant 20200671, Grant 20201203, and Grant 20201623; in part by the Consejo Nacional de Ciencia y Tecnología (Proyecto Apoyado por el Fondo Sectorial de Investigación para la Educación), Mexico, under Grant A1-S-24762, and in part by the Ministerio de Ciencia, Innovación y Universidades (MCIyU), Spain, under Grant PGC2018-096265-B-I00.

ABSTRACT Departing from analyzing a general input-saturated second-order system, a Lyapunov-based constructive procedure for the output-feedback stabilization of the constantly perturbed DC-DC buck power converter is presented. The proposed scheme also incorporates a Σ−Δ modulator. The obtained control scheme is developed in two parts: a proportional-integral-type family of algorithms devoted to regulating the uncertain system by using measurements of the output voltage and a Σ−Δ modulator dedicated to transforming the control action into a {0, 1} discrete-valued signal. This modulator is a kind of a sliding controller, which can be seen as a subsystem with an on-off output. This combination, the PI–type family of controllers and the Σ−Δ modulator, assures the global stability of the closed-loop system, even if parametric uncertainties are presented. The convergence analysis was carried out using Lyapunov's method. The theoretical results are confirmed using real–time experimental tests, which demonstrate the anti-windup scheme and the Σ−Δ modulator efficiency. The experiments consider the saturation of the control input and disturbances, having obtained convincing results.

INDEX TERMS DC-DC buck converter, Lyapunov's method, saturation control, Σ−Δ modulator, experimental results.

I. INTRODUCTION

Direct current to direct current (DC-DC) power converters have been used for a long time and remain valid because new applications continue to appear [1], particularly those related to clean energies. For example, DC-DC power converters are used in electric traction of trolleys [2]. Another common application can be found in uninterrupted power supplies where DC-DC power converters are the main circuit of such devices. Because the main virtue of these converters is voltage regulation, several electronic gadgets make use of them. For instance, the USB ports found in personal computers or smartphones allow connecting peripherals that draw power, which needs to be regulated. Furthermore, battery chargers, microprocessors, and motherboards, extensively use DC-DC converters. Electronic devices that need constant voltage to safely and correctly function are supplied with battery packages (for details, refer to the following works and the references therein [15], [16], [17], [18]). In this situation, buck converters are appropriate since the output voltage is regulated to a lower voltage than the supplied by the batteries. Consequently, control schemes should be improved to meet the needs of these pervasive devices.

Recently, efficient control strategies have been designed for several types of power converters. A discontinuous control method was applied in [3] and [4] to compensate for disturbances in a buck power converter. In [5], a control design was given in order to ensure that the current constraints are not violated at any time in the presence of disturbances. A high-order sliding mode controller was applied to the buck

The associate editor coordinating the review of this manuscript and approving it for publication was Sun Junwei.

converter in [6]. The control of a triple input DC-DC converter was discussed in [7], where the application of fuzzy logic was crucial. In the work [8], the authors introduced a passivity-based control scheme for regulating the voltage of a DC microgrid through boost converters. In [9], the authors considered a fractional-order PID-type controller for a boost converter. In [10], an output reference trajectory tracking controller was proposed, which can be applied to a large class of systems, including power converters.

The input saturation frequently appears when more power than the one that can be dissipated is demanded to the system. In other words, all physical systems are constrained to input saturation. The duty cycle is the natural control input of the DC-DC power converters. However, due to several factors such as limitations in designed circuitry, the lower and higher input limits can be higher than 0% and lower than 100%, respectively. See, for example, [11], [12], [13], [14]. Actually, the saturation of the duty cycle in power converters appears in the circuitry that enables the transistor gate. It is worth noticing that only a few controllers for input-saturated power converters with rigorous closed–loop stability analysis have been given in the literature. In [19], oscillations were studied in voltage-mode PID-type digitally controlled converters with asymmetric saturation in the duty cycle. The control of boost power converters in microgrids with input limitations was studied in [20]. In [21], the authors introduced a method to avoid duty cycle saturation during the startup in the bidirectional buck-boost converters. The combination of a photovoltaic plant with a two-cell buck converter with input saturation was analyzed in [22]. In [23], the maximum power from a photovoltaic array is obtained, taking into account input constraints of a boost DC-DC converter. In [24] and [25], observers for a saturated control law were analyzed in order to regulate the output voltage of a boost power converter.

On the other hand, the most common strategies used in industry to regulate DC-DC power converters are those based on proportional (P) control, proportional-integral (PI) control and proportional-integral-derivative (PID) control [26], [27]. Besides, controllers derived from the flatness approach have been proven to be very robust and efficient as shown in [28], [29], [30], [16], [31] and [32]. However, more advanced control approaches should be applied when natural restrictions of the system are considered in the presence of either internal or external non-modeled dynamics. A common solution used to counteract the effect of such input perturbation consists in proposing a controller based on the average models of switched systems [33]. Once the controller has been proposed, either a pulse width modulation system or a Σ–Δ modulator should be used to implement the control task over the switched system.

Let us notice that Σ–Δ modulators have been extensively used in analog signal encoding and, in combination with a control strategy, they may provide better performance in comparison with the standard pulse width modulator [34], [35]. The application of Σ–Δ modulators in rigorous Lyapunov-based control design still deserves study and consideration, particularly if practical applications are made. In the case of power converters, the Σ–Δ modulation block translates the continuous controller output into a {0, 1} signal for the transistor gate.

As mentioned earlier, when continuous control laws are designed for the averaged system, the situation in that the input is restricted to a specific range must always be considered.

Under the described scenery, the output voltage control is even more complicated either if the input voltage is uncertain or if the inductor current is unmeasurable.

Concerning the literature review, the design of controllers in combination with $\Sigma-\Delta$ modulation for the input-saturated system seems to be new.

The contributions of this manuscript are explained as follows:

- The output stability of a DC-DC buck power converter subjected to input and disturbances constraints is given. As mentioned, the solution to this control problem requires more sophisticated techniques. First, a general second-order system with input constraints, a PI-type controller, and the stability of the resulting closed–loop system are analyzed.
- Derived from the general case, our strategy to regulate the input-constrained averaged DC-DC buck power converter consists of a Lyapunov-based PI-type controller and the Σ–Δ modulator, acting as a sliding controller, which transforms the averaged input into a discrete set {0, 1} signal directly applicable to the transistor gate.
- An extensive real–time experimental study is provided. In particular, cases of the proposed PI-type family of controllers, the simple PI scheme and the PI with anti–windup control are experimentally tested under several operation conditions, including disturbances. Results indicate that the latter one presents the best performance concerning the settling time and percentage overshoot. Besides, the controllers are tested by using the classical pulse width modulation (PWM) technique and the $\Sigma-\Delta$ modulation.

The difference of this manuscript with respect to previous research is that refinements in the development of the Lyapunov function and stability conditions are provided. In addition, for the first time, the rigorous proof of the asymptotical stability for PI-type controllers with Σ–Δ modulator applied to an input–constrained buck converter is established.

The remaining of this work is organized as follows. In Section II, the problem statement is introduced. For a general input-saturated second-order system, the family of PI–type controllers, Lyapunov's stability analysis, and the needed Σ–Δ modulator are described in Section III. The application of the proposed controllers to the DC-DC buck power converter and the closed–loop stability are discussed in Section IV. In Section V, the results of experimental implementations in a microcontroller and a buck power converter

are described. Finally, concluding remarks are presented in Section VI.

II. PROBLEM STATEMENT

Consider the following second-order system:

$$\lambda_2\ddot{x} + \lambda_1\dot{x} + \lambda_0 x = v + \delta, \tag{1}$$

where $\{\lambda_1 > 0, \lambda_2 > 0, \lambda_0 \geq 0\}$ are the set of system parameters, δ is a partially known external perturbation, and v is the system saturated input as follows:

$$v = \sigma[u] = \begin{cases} \overline{u}, & \text{for } u > \overline{u}, \\ u, & \text{for } \underline{u} \leq u \leq \overline{u}, \\ \underline{u}, & \text{for } u < \underline{u}, \end{cases} \tag{2}$$

with $\underline{u} < \overline{u}$. The position error is defined as:

$$e = x - x_d,$$

where x_d is a desired constant reference. Then, the control problem consists in designing a continuous controller u, to render the position error to zero, assuming that:

$$\underline{u} < u_s \widehat{=} \lambda_0 x_d - \delta < \overline{u}, \tag{3}$$

and this error is always available for measurements. In the forthcoming developments the definitions

$$I = [\underline{u}, \overline{u}] \text{ and } I_0 = (\underline{u}, \overline{u})$$

are used with $\underline{u} < \overline{u}$.

Even when the formulation of this control problem seems easy to solve, it is a challenging task because the system is continuously perturbed, and the control is restricted. Finally, no restriction on the sign of $\underline{u}$ and $\overline{u}$ is imposed.

Remark 1: Please note that the point $(x(t) = x_d, v(t) = u_s)$ is a solution of the closed-loop (1).

III. A GENERAL CONTROL STRATEGY

In this section, a family of PI-type controllers is designed. The introduced control algorithms allows solving the problem mentioned above. A lemma helpful for the closed-loop system analysis is revisited. Afterwards, through a detailed analysis based on Lyapunov's theory, conditions for convergence of the closed-loop error trajectories are given.

To shape the needed Lyapunov function, which allows proposing a PI-type controller with anti-windup, a lemma taken from [43] is recalled and proven.

Lemma 1: Under assumption (3), the point $u = u_s$ is the single minimum of the function H(u):

$$H(u) = \int_0^u \sigma[s]ds - u_s u + \frac{u_s^2}{2}. \tag{4}$$

Besides, $H(u)$ is strictly positive and radially unbounded, with $H(u_s) = 0$.

Proof: From *(4)*, the function $H(u)$ is explicitly given by:

$$H(u) = \frac{u_s^2}{2} + \begin{cases} \overline{u}u - \dfrac{\overline{u}^2}{2}, & \text{for } u > \overline{u}, \\ \dfrac{1}{2}u^2 - u\,u_s, & \text{for } \underline{u} \leq u \leq \overline{u}, \\ \underline{u}u - \dfrac{\underline{u}^2}{2}, & \text{for } u < \underline{u}. \end{cases} \tag{5}$$

Notice that $H(u_s) = 0$. Next, from the definition of $H(u)$, given in (*4*), the following is satisfied:

$$H^{'}(u) = \sigma[u] - u_s. \tag{6}$$

Therefore, $H^{'}(u) = 0$, implying, according to *(3)*, that $u = u_s$ is a single critical value. On the other hand, since:

$$\frac{d^2H(u)}{du^2} = 1,$$

for all $u \in (\underline{u}, \overline{u}) = I_0$, $u = u_s$ is the single minimum inside of I_0. That is, u_s is a minimum with $H(u_s) = 0$ and $H(u) > 0$, for all $u \in I_0/u_s$. It only remains to show that $H(u)$ is strictly positive definite and radially unbounded, for all $u \notin I_0$. Thus, to see the positiveness of $H(u)$ for $u \notin I_0$, two cases must be analyzed.

i) $u > \overline{u}$, according to (5) and (4):

$$H(u) = (\overline{u} - u_s)u - \frac{\overline{u}^2}{2} + \frac{u_s^2}{2} > 0. \tag{7}$$

ii) Complementarily, when $u < \underline{u}$:

$$H(u) = (\underline{u} - u_s)u - \frac{\underline{u}^2}{2} + \frac{u_s^2}{2} > 0. \tag{8}$$

The positiveness of expressions (7) and (8), and the fact that $H(u)$ is radially unbounded can be found in the appendix.

Please note that function $H(u)$ helps us to generate a family of PI-type controllers with anti-windup. Also, this function allows to solve the above introduced control problem.

Shaping the family of PI-type controllers:

The following PI-type control law is proposed:

$$u = -k_P e - k_I z, \tag{9}$$

where constants k_P and k_I are strictly positive, and z is a filtered signal proposed as:

$$\dot{z} = e + k_A \phi(u), \tag{10}$$

where $k_A > 0$, and ϕ is a suitable nonlinear function selected, such that:

$$(\sigma[u] - u_s)\,\phi(u) \geq 0 \quad \forall \quad u \in \Re. \tag{11}$$

Remark 2: *It is easy to see that, under the assumption (3) the following inequality holds:*

$$(\sigma[u] - u_s)\,dzn[u] \geq 0 \quad \forall \quad u \in \Re,$$

where the dead-zone is defined as $dzn[u] = u - \sigma[u]$. As a matter of fact $(\sigma[u] - u_s)\,dzn[u] = 0$ if and only if $u \in I$. That is, $\phi(u) = u - \sigma[u]$.

From the expression (1), the dynamic error equation for e is given by:

$$\ddot{e} = -\frac{\lambda_1}{\lambda_2}\dot{e} - \frac{\lambda_0}{\lambda_2}e + \frac{1}{\lambda_2}\left(\sigma[u] - u_s\right), \tag{12}$$

where u_s was previously defined in (3).

The conditions for the stability of the equilibrium of the system (12)-(2) in closed-loop with the controller (9) and (10) should be found. With this aim, consider the following function:

$$V(X) = \frac{1}{2}\left(\beta_0 e^2 + 2\beta_1 e\dot{e} + \beta_2 \dot{e}^2\right) + \beta_3 H(u), \tag{13}$$

where $X = (e, \dot{e}, u) \in R^3$ is the state vector, and β_0, $\beta_1\beta_2$, β_3 are strictly positive constants, and $H(u)$ is the continuous and differentiable function expressed in equation (4). First, observe that $V(X)$ can be rewritten as

$$V(X) = \frac{1}{2}\begin{bmatrix} e \\ \dot{e} \end{bmatrix}^T P \begin{bmatrix} e \\ \dot{e} \end{bmatrix} + H(u),$$

where

$$P = \begin{bmatrix} \beta_0 & \beta_1 \\ \beta_1 & \beta_2, \end{bmatrix}$$

is positive definite if

$$\Delta = \beta_0\beta_2 - \beta_1^2 > 0, \tag{14}$$

in agreement to Silvester's criterion. Besides, $H(u)$ in (4) is a positive definite and radially unbounded function, as shown in Lemma 1. The function $H(u)$ has global minimum at $u = u_s$, which at the same time implies that $V(X)$ has a global minimum at $X_s = (0, 0, u_s)$. Finally, notice that the change of the coordinates

$$X = \begin{bmatrix} e \\ \dot{e} \\ u \end{bmatrix} = \begin{bmatrix} 1 & 0 & 0 \\ 0 & 1 & 0 \\ -k_P & 0 & -k_I \end{bmatrix} \begin{bmatrix} e \\ \dot{e} \\ z \end{bmatrix}$$

is globally invertible. Therefore, the given arguments are sufficient to claim that by construction $V(X)$ in (13) qualifies as a Lyapunov function candidate for the equilibrium point X_s of the closed-loop system (1), (9) and (10).

Inequalities (18) and (19), introduced below, give sufficient conditions related with the physical parameter to assure the positiveness of inequality (14), which in turn assures the positiveness of V.

Therefore, the time derivative of (13) satisfies the following equality:

$$\dot{V}(X) = \beta_0 e\dot{e} + \beta_1\dot{e}^2 + \left(\beta_1 e + \beta_2\dot{e}\right)\ddot{e} + \beta_3\left(\sigma[u] - u_s\right)\dot{u}. \tag{15}$$

Now, from (9) and (10), the equation

$$\dot{u} = -k_P\dot{e} - k_I\left(e + k_A\phi(u)\right), \tag{16}$$

holds. Hence, after substituting the values of (12) and (16) into the equation (15) the following is obtained:

$$\begin{aligned}\dot{V}(X) = \dot{e}^2\left(\beta_1 - \frac{\beta_2\lambda_1}{\lambda_2}\right) - \frac{\beta_1\lambda_0}{\lambda_2}e^2 \\ -\beta_3 k_A k_I\left(\sigma[u] - u_s\right)\phi(u) \\ +e\dot{e}M_1 + \left(eM_2 + \dot{e}M_3\right)\left(\sigma[u] - u_s\right),\end{aligned}$$

where

$$\begin{aligned}M_1 &= \beta_0 - \frac{\beta_2\lambda_0}{\lambda_2} - \frac{\beta_1\lambda_1}{\lambda_2}, \\ M_2 &= -\beta_3 k_I + \frac{\beta_1}{\lambda_2}, \\ M_3 &= -\beta_3 k_p + \frac{\beta_2}{\lambda_2}.\end{aligned}$$

From the above, the constants β_0, β_1, β_2, β_3 and β_4 should be defined such that:

$$\begin{aligned}\beta_1 - \frac{\beta_2\lambda_1}{\lambda_2} = -1, \quad M_1 = 0, \\ M_2 = 0, \quad M_3 = 0.\end{aligned}$$

It is easy to see, after some algebraic manipulations, that:

$$\begin{aligned}\beta_0 &= \frac{k_p\lambda_0 + k_I\lambda_1}{\left(k_p\lambda_1 - k_I\lambda_2\right)}, \quad \beta_1 = \frac{k_I\lambda_2}{k_p\lambda_1 - k_I\lambda_2}, \\ \beta_2 &= \frac{k_p\lambda_2}{\left(k_p\lambda_1 - k_I\lambda_2\right)}, \quad \beta_3 = \frac{1}{\left(k_p\lambda_1 - k_I\lambda_2\right)},\end{aligned} \tag{17}$$

where $k_p\lambda_1 - k_I\lambda_2 > 0$, because as it was already mentioned, β_2 is positive. It implies that:

$$k_p > k_I\lambda_2/\lambda_1. \tag{18}$$

After substituting the obtained values of $\{\beta_0, \beta_1, \beta_2\}$ into the inequality (14),

$$\Delta = \frac{k_p\lambda_0 + k_I(k_p\lambda_1 - k_I\lambda_2)}{\left(k_p\lambda_1 - k_I\lambda_2\right)^2}, \tag{19}$$

which, according to (18), is positive. Hence, selecting $\phi(u) = dzn[u]$, and considering that the set of parameters β_i with $i = \{0, 1, 2, 3\}$ satisfy (17) with $k_p > k_I\lambda_2/\lambda_1$, then the equation (15) can be read as:

$$\begin{aligned}\dot{V}(X) = -\dot{e}^2 - \frac{k_I\lambda_0}{k_p\lambda_1 - k_I\lambda_2}e^2 \\ - \beta_3 k_A k_I\left(\sigma[u] - u_s\right)dzn[u].\end{aligned} \tag{20}$$

Now, according to remark 2, the function $\dot{V}(X)$ is negative semidefinite if $\lambda_0 > 0$. Application of Barbalat's lemma completes the proof that the solutions $(e(t), \dot{e}(t))$ converge to zero for any initial condition.

The other interesting case is when $\lambda_0 = 0$ and the equation (20) reads as:

$$\dot{V}(X) = -\dot{e}^2 - \beta_3 k_A k_I\left(\sigma[u] - u_s\right)dzn[u].$$

The fact that $\dot{V} \leq 0$, for all X, implies the stability of the equilibrium $(0, 0, u_s)$ in the Lyapunov's sense. That is, signals $\{e, \dot{e}, u\} \in L_\infty$. To complete the proof, LaSalle's invariance theorem is applied. For this end, the following set is defined:

$$S = \{(e, \dot{e}, u) : \dot{V} = \dot{e}^2 + \beta_3 k_A k_I\left(\sigma[u] - u_s\right)dzn[u] = 0\}.$$

Now, the largest invariant set $\Theta \subset S$ should be found. A solution starting at S satisfies $\dot{e} = 0$ and $u \in I$, according to the remark 2. It also implies that $\ddot{e} = 0$ and $e = \bar{e}$, where $\bar{e}$

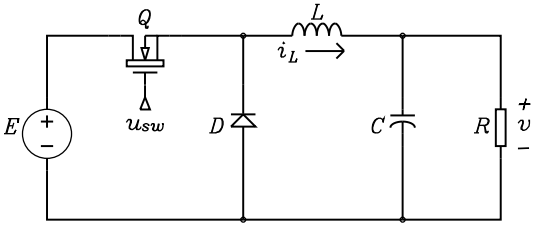

FIGURE 1. DC-DC buck power converter.

is a fixed constant in the set S. Substituting these values into the equation (12), the equation

$$0 = (\sigma[u] - u_s),$$

is obtained, which implies that $u = u_s$ and $\dot{u} = 0$ in the set S. Finally, substituting these values into the expression of $\dot{u}$ given in (16), and considering that $u \in I$, the relationship $0 = -k_I e$ is obtained implying that $e = 0$. From this analysis, the largest invariant set contained in S is constituted by the set $\Theta = \{e = 0, \dot{e} = 0, u = u_s\}$. Then, according to LaSalle's invariance theorem, all trajectories of the closed-loop system asymptotically converge towards the invariant set contained in $\Theta \subset S$, which is constituted by the equilibrium point Θ.

The previous discussion is summarized in Proposition 1.

Proposition 1: *Consider the system (1) restricted to* $\{\lambda_1 > 0, \lambda_2 > 0, \lambda_0 \geq 0\}$*, and under the assumption (3), in closed loop with the PI-type controller, formed by the equations (2), (9) and (10), with:*

$$\phi(s) = s - \sigma[s].$$

Then, errors e *and* $\dot{e}$ *asymptotically converge to the origin, if the control gains are selected such that:*

$$k_p > k_I \frac{\lambda_2}{\lambda_1}, \quad k_A > 0.$$

In the next section, the effectiveness of the family of PI-type controllers is applied to the stabilization of the well-known DC-DC buck power converter.

IV. DC-DC BUCK CONVERTER: A PRACTICAL APPLICATION

In this section, the above introduced PI-type controllers is applied to control the average DC-DC buck power converter. This system, shown in Figure 1, consists of a power supply, an inductor, a capacitor, a resistive load, a diode, and a transistor. The buck power converter mathematical model, assuming that it operates under the continuous conduction mode, is given by [29], [36], [37]:

$$\begin{aligned} L\frac{di}{dt} &= -v + Eu_{sw} + d_1, \\ C\frac{dv}{dt} &= i - \frac{v}{R} + d_2, \end{aligned} \tag{21}$$

where i represents the inductor current, v the output capacitor voltage, and u_{sw} is a discrete function that takes values in the set $\{0, 1\}$ and governs the switch position (control input), L is the inductance of the input circuit, C is the capacitance of the output filter, R is the output load resistance, and E is the external voltage supply. Additionally, the small constant perturbations d_1 and d_2 are considered. It is well-known that the corresponding average model is represented by the same system (21) if the discrete function u is substituted by a sufficiently smooth function u_{av}, taking values in the compact interval of the real line $[0, 1]$. In other words, the average model is represented by the following system of equations:

$$\begin{aligned} L\frac{di}{dt} &= -v + Eu_{av} + d_1, \\ C\frac{dv}{dt} &= i - \frac{v}{R} + d_2. \end{aligned} \tag{22}$$

It should be noticed that other type of perturbations and uncertainties could have been taken into account such as the parasitic resistance of the capacitor. However, the control of DC-DC buck power converters with parasitic elements and input nonlinearity is an interesting topic but not much addressed in the literature because of the complexity of the resulting models. Thus, the consideration of that type of models under input limitations is left aside.

Since the changes in the system parameter due to aging are very slow, they could be interpreted as additive constant disturbances. The system (22) is subject to additive constant perturbations. Thus, it is expected that the proposed controller behaves in an efficient manner achieving the control goal of output voltage regulation. In other words, the provided analysis considers the presence of disturbances, which do not affect the output voltage regulation. Studies addressing the control of the DC-DC buck power converter without input limitations and considering that the parameters are perturbed are in [38] and [39], for example. However, other more sophisticated approaches [40], [41], can be adapted to regulate the output voltage.

Remark 3: *According to [34], in the case of* $d_1 = d_2 = 0$ *the steady state of* i *and* v*, which is associated with the average model (22), for a constant control* $u_{av} = U$ *is determined by* $i = v/R$ *and* $v = EU$*. Consequently, as* $U \in [0, 1]$ *the buck power converter output voltage is restricted to* $0 \leq v \leq E$*. Due to this fact, this topology is known as the step-down converter.*

It is possible to prove that the system (21) can be written in the structure of the generalized system (1). With this in mind, the time derivative of the capacitor current $i_C = C\dot{v}$ is computed as follows

$$\frac{d}{dt}i_C = \frac{d}{dt}C\dot{v} = C\ddot{v} = \dot{i} - \dot{v}/R + \dot{d}_2. \tag{23}$$

By substituting the inductor current dynamics Ldi/dt (see equation (22)) into the expression (23) and considering that $\dot{d}_2 = 0$, the following second-order linear equation is obtained:

$$\frac{LC}{E}\ddot{v} + \frac{L}{ER}\dot{v} + \frac{1}{E}v = u_{av} + d, \tag{24}$$

with $d = d_1/E$. Now, if the voltage error is defined as:

$$e_v = v - v_d,$$

then the dynamic error equation is given by:

$$\frac{LC}{E}\ddot{e}_v + \frac{L}{ER}e_v + \frac{1}{E}e_v = u_{av} + d - \frac{v_d}{E}, \tag{25}$$

with the following natural restrictions:

$$0 \leq u_{\min} < u_s = d - \frac{v_d}{E} < u_{\max} \leq 1. \tag{26}$$

That is, $u_s \in (u_{\min}, u_{\max}) \subset (0, 1)$, and $u_{av} \subset [0, 1]$. Hence, it is easy to see that the system (25), restricted by (26), can be stabilized if Proposition 1 is applied by noting $\underline{u} = u_{\min}$, $\overline{u} = u_{\max}$, etc.

It is noteworthy to mention that in the absence of input constraints, the system (25) is easy to control. However, the system (25) becomes nonlinear and complex if the control input is affected by a hard saturation nonlinearity. In this situation, the system (25) is physically restricted with (26) and $u_{av}(t) \in [0, 1]$ and cannot be stabilized by using a linear PI-controller with arbitrary gain selection. In other words, stability is attained along as a special relation of control gains is achieved and integrator anti-windup is incorporated. These considerations are formalized in the following.

Proposition 2: *Consider the system (25) with its corresponding saturated function defined as:*

$$u_{av} = \sigma[u] = \begin{cases} u_{\max} & \text{for } u > u_{\max}, \\ u & \text{for } u_{\min} \leq u \leq u_{\max}, \\ u_{\min} & \text{for } u < u_{\min}, \end{cases}$$

under the assumption that $u_s \in (u_{\min}, u_{\max}) \subset (0, 1)$. *Then, the following PI-type controller:*

$$\begin{aligned} u &= -k_P e_v - k_I z, \\ \dot{z} &= e_v + k_A(u - \sigma[u]), \end{aligned} \tag{27}$$

where the set of constants $\{k_p, k_I, k_A\}$ *are strictly positive and restricted to*

$$k_p > k_I RC, \tag{28}$$

ensures that $(e_v, \dot{e}_v)$ *asymptotically converge to zero.*

The corresponding proof is omitted because it is evidently a direct consequence of Proposition 1.

The only condition required to ensure convergence of the voltage error $e_v(t)$ is the inequality (28). Notice that if slow variations of the resistance R and the capacitance C were presented, the closed-loop stability will still be kept under the condition (28), which at the same time does not involve the value of the inductance L. These advantages makes the controller (27) an excellent choice in the situation that the values of the buck power converter components change either by aging or temperature.

The controller (27) corresponds to the well-known PI-control with back calculation anti-windup [42], [43], and that has been applied in others works [43], [44]. However, in the study presented in this manuscript, a different Lyapunov function is used to prove stability, having the advantage that a more general result is obtained, as shown in Proposition 1.

A. THE $\Sigma-\Delta$ MODULATOR

$\Sigma-\Delta$ modulation is an important tool that allows the translation of continuous (*i.e.*, average) input signals into sign valued, or finite set-valued, output signals with preserved equivalent average behaviors. It is worthy to mention that the use of $\Sigma-\Delta$ modulation in sliding mode control of linear and nonlinear systems has been explored in [34].

In the seminal textbook [45], several developments connected with analog-to-digital conversion systems are found. In that regard, the sliding mode implementation for the proposed PI-type average controller u_{av} using the $\Sigma-\Delta$ modulator is accomplished by following the method introduced in [34]. So, the next filter:

$$\begin{aligned} \dot{\xi} &= \sigma[u] - u_{sw}, \\ u_{sw} &= \frac{1}{2}(1 + sign[\xi]), \end{aligned} \tag{29}$$

where u_{av} was defined according to Proposition 2, assures the implementation of the actual controller u_{sw}, that acts on the switching system (21). Next, a theorem introduced in [35] is transcribed, where sufficient evidence to justify the above is given.

Theorem 1: Consider the $\Sigma-\Delta$ -modulator of equations (29). Given a sufficiently smooth, bounded, signal u_{av}, then the integral error signal, $\xi(t)$, *converges to zero in a finite time,* $t_h > 0$. *Moreover, from any arbitrary* $\xi(t_0)$, *a sliding motion exists on the perfect encoding condition surface, represented by* $\xi = 0$, *for all* $t > t_h$, *provided the following condition is satisfied for all* t:

$$0 < u_{av}(t) < 1. \tag{30}$$

The proof of Theorem 1 can be found in [34], [35].

A block diagram implementation of the PI-type controller (27), the $\Sigma-\Delta$ modulator (29) in closed–loop with the buck power converter is illustrated in Figure 2. As will be shown later, experimental evidence has been found on the efficiency of controllers implemented with the $\Sigma-\Delta$ modulator (29).

Remark 4: *Inserting a state variable* $\Sigma-\Delta$ *-modulator, as a transducer for the analog input signals* u_{av}, *into the discrete output signals* u_{sw}, *causes the ideal sliding dynamics to coincide with the average designed closed-loop behavior, as long as an average feedback controller is available for the average model of a switched plant (the interested reader can find the corresponding formal justification in [34], [35]). Figure 2 illustrates the representation of the* $\Sigma-\Delta$ *-modulator together with the proposed average controller* u_{av}. *Finally, according to Proposition 1, the restriction (30) is always fulfilled as long as the previously defined uncertainty* $u_s \in (0, 1)$. *Conversely, if the latter does not hold, evidently, there does not exists a controller* u_{sw} *that, in closed-loop with the system in (24), ensures that the voltage position error* e_v *converges to zero.*

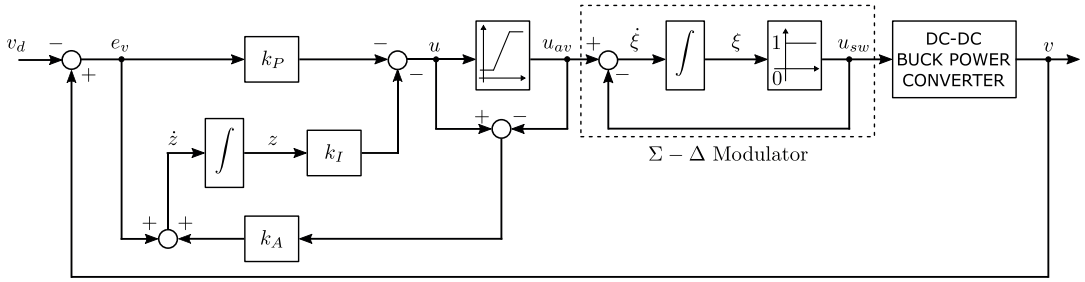

FIGURE 2. Block–diagram implementation of the PI-type scheme in (27) which incorporates the Σ − Δ modulator (29).

V. EXPERIMENTAL RESULTS

A. PLATFORM DESCRIPTION

Controllers are implemented in the TMS320F28379D Delfino microcontroller using the low cost Delfino Launchpad. The sample rate used in the microcontroller is 100 kHz. Matlab-Simulink is linked to *Code Composer Studio* to embed and implement the controller. Simulink enables to generate C code and a real-time executable and download it to the Launchpad. Serial communication is used between Simulink and the Delfino Launchpad to monitor and obtain the experimental results of the control signal u_{av} and the the voltage signal v.

The experimental buck converter uses an FDPF085N10A N-channel MOSFET and a MBR1050 Schottky diode. The 6N137 optocoupler is used to drive the MOSFET. Two MCP602 operational amplifiers and one ISO224 isolated amplifier are implemented to condition the output voltage v in order to be measured by the microntroller. See Figure 3 for a detailed description of the experimental platform used for implementing controllers in real-time.

The data sheets of the manufacturers show that the bandwidth of the components used in the experimental platform is sufficiently large to work efficiently for all the operation conditions to be described in each set of results.

The values of the the buck parameters are $L = 200$ [mH], $C = 220$ [μF], and $R = 200$ [Ω]. The supply voltage E is switched between 20 [V] and 8 [V] at different time intervals by using relay circuits.

B. CONDITIONS OF EXPERIMENTAL COMPARISONS

The two controllers are tested in four different conditions. The first scheme corresponds to the simple PI controller, which results from (9)–(10) with $\phi(u) = 0$. The second algorithm is the PI anti-windup controller (27), which as mentioned before is obtained from (9)–(10) but with $\phi(u) = dzn(u)$. Hereafter, the controller (27) will be denoted as PIAW.

Four sets of experiments are presented. Experiments 1 to 3 are implemented by using the Σ−Δ modulator. Experiment 4 consists in implementing the PI and PIAW controllers using the Σ−Δ modulator and the PWM technique. In other words, the performance of the controllers is tested by using different modulation schemes to enable the MOSFET gate.

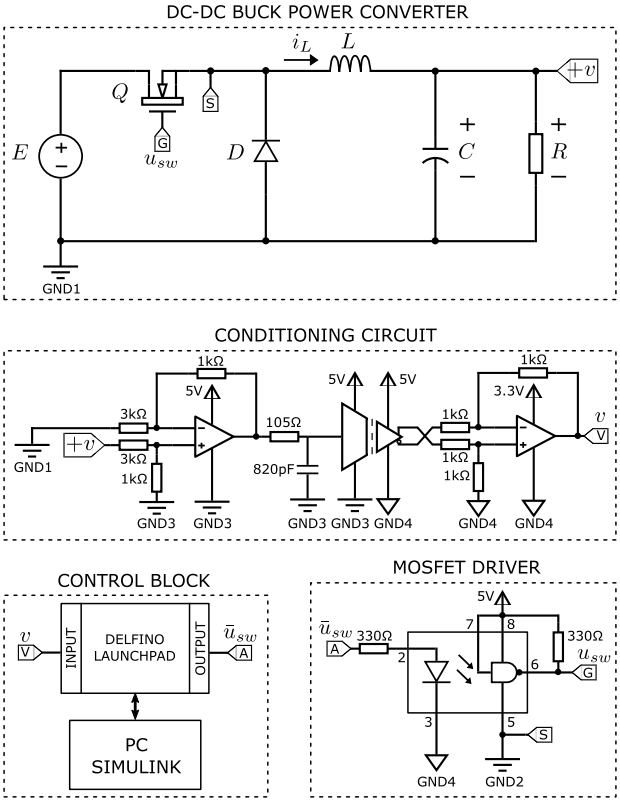

FIGURE 3. Experimental platform.

TABLE 1. Experiment 1: Changes in desired output voltage v_d, supply voltage E, and load resistance R for different time intervals.

Time Range	v_d	E	R
$0 \leq t < 0.5$ [s]	5 [V]	20 [V]	200 [Ω]
$0.5 \leq t < 1$ [s]	5 [V]	8 [V]	94 [Ω]
$1 \leq t < 1.5$ [s]	10 [V]	20 [V]	94 [Ω]

C. EXPERIMENT 1: PERFORMANCE UNDER DISTURBANCES

The PI and PIAW controllers are tested experimentally by changing the desired voltage v_d, supply voltage E, and load resistance R at the same time. This experiment is useful to appreciate the response of the controller under load resistance variation. The changes are described in Table 1. For both experiments, the initial output voltage is $v(0) = 10$ [V]. The

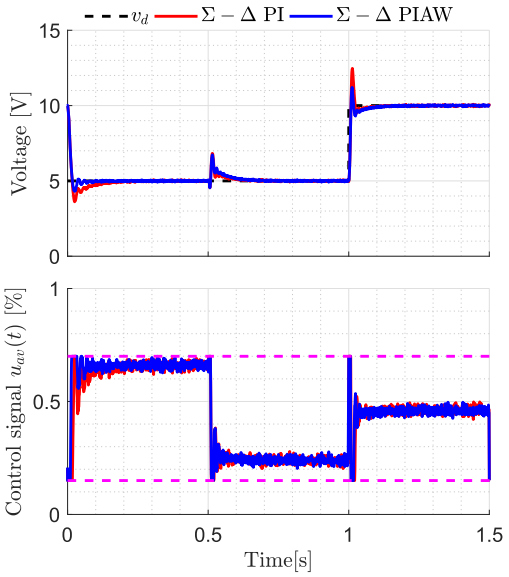

FIGURE 4. Experiment 1: Time evolution of the voltage $v(t)$ and control action $u_{av}(t)$.

TABLE 2. Experiment 1: Settling time and percentage overshoot of the output voltage $v(t)$ in different time periods.

	Settling time		
Time Range	PI	PIAW	Improvement
$0 \leq t < 0.5$ [s]	0.05479 [s]	0.02968 [s]	45.82 %
$0.5 \leq t < 1$ [s]	0.5345 [s]	0.5453 [s]	−1.98 %
$1 \leq t < 1.5$ [s]	1.019 [s]	1.013 [s]	0.58 %

	Percentage overshoot	
Time Range	PI	PIAW
$0 \leq t < 0.5$ [s]	−27.7 %	−13.64 %
$0.5 \leq t < 1$ [s]	36.52 %	34.6 %
$1 \leq t < 1.5$ [s]	24.7 %	12 %

saturation limits are $u_{min} = 0.15$ and $u_{max} = 0.70$. The PI and PIAW controllers are implemented using gains $k_P = 0.45$ and $k_I = 10$. The PIAW uses the same gains and $k_A = 10$. The results are observed in Figure 4, which shows the time evolution of the output voltage $v(t)$ and control actions $u_{av}(t)$. Notice that during the transients, the PIAW behaves much better since the settling time and percent overshoot are much smaller than the ones given by the PI controller. The performance comparison is explicitly given in Table 2. By using the PIAW the percentage overshoot is drastically improved for all time ranges where the desired voltage v_d, supply voltage E, and load resistance R are changed.

D. EXPERIMENT 2: PERFORMANCE IN PURE OUTPUT TRACKING

While the supply voltage E is constant for all time, this experiment considers that the desired voltage v_d is changed suddenly from a value to another in different time ranges. This is commonly known as an output tracking experiment. See Table 3 for the description of the desired voltage values v_d

TABLE 3. Experiment 2: Changes in the desired output voltage v_d for different time intervals.

Time Range	v_d
$0 \leq t < 0.5$ [s]	6 [V]
$0.5 \leq t < 1$ [s]	3 [V]
$1 \leq t < 1.5$ [s]	12 [V]

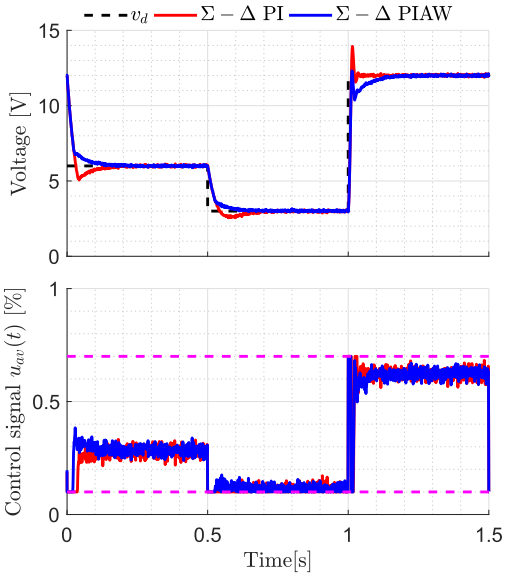

FIGURE 5. Experiment 2: Time evolution of the voltage $v(t)$ and control action $u_{av}(t)$.

TABLE 4. Experiment 2: Settling time and percentage overshoot of the output voltage $v(t)$ in different time periods.

	Settling time		
Time Range	PI	PIAW	Improvement
$0 \leq t < 0.5$ [s]	0.06703 [s]	0.05001 [s]	25.39 %
$0.5 \leq t < 1$ [s]	0.6224 [s]	0.5682 [s]	8.72 %
$1 \leq t < 1.5$ [s]	1.018 [s]	1.029 [s]	−1.06 %

	Percentage overshoot	
Time Range	PI	PIAW
$0 \leq t < 0.5$ [s]	−15.56 %	0 %
$0.5 \leq t < 1$ [s]	−14.7 %	0 %
$1 \leq t < 1.5$ [s]	16.16 %	2.58 %

in different time ranges. The initial output voltage is $v(0) = 12$ [V]. The saturation limits are $u_{\min} = 0.1$ and $u_{\max} = 0.7$. The PI controller is implemented using gains $k_P = 0.45$ and $k_I = 10$. The PIAW uses the same gains and $k_A = 5$. The supply voltage E is kept constant at 20 [V]. The time evolution of the output voltage $v(t)$ and control input $u_{av}(t)$ are depicted in Figure 5. Similarly to Experiment 2, at first sight the PIAW scheme seems to present the best performance since the settling time and percentage overshoot are much smaller than the ones obtained with the PI controller. The performance indexes are explicitly computed and shown in Table 4. Notice that for all the time ranges the desired voltage v_d is changed, the PIAW scheme behaves the best.

TABLE 5. Experiment 3: Changes in desired voltage v_d for different time intervals.

Time Range	v_d
$0 \leq t < 0.5$ [s]	5 [V]
$0.5 \leq t < 1$ [s]	0 [V]
$1 \leq t < 1.5$ [s]	14 [V]

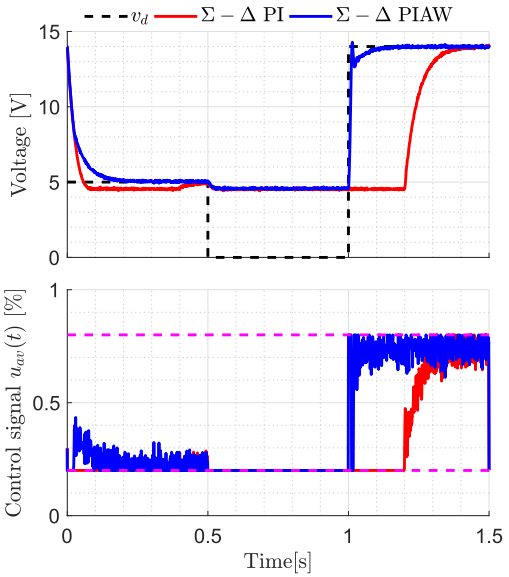

FIGURE 6. Experiment 3: Time evolution of the voltage $v(t)$ and control action $u_{av}(t)$.

TABLE 6. Experiment 3: Settling time and percentage overshoot of the output voltage $v(t)$ in different time periods.

	Settling time		
Time Range	PI	PIAW	Improvement
$0 \leq t < 0.5$ [s]	0.4001 [s]	0.122 [s]	69.50 %
$0.5 \leq t < 1$ [s]	–	–	–
$1 \leq t < 1.5$ [s]	1.29 [s]	1.01 [s]	21.70 %

	Percentage overshoot	
Time Range	PI	PIAW
$0 \leq t < 0.5$ [s]	10%	0%
$0.5 \leq t < 1$ [s]	–	–
$1 \leq t < 1.5$ [s]	0%	4%

E. EXPERIMENT 3: PERFORMANCE UNDER AN INPUT FAULT

This set of experiments consists in observing the performance of the PI and PIAW algorithms in the situation where the desired voltage v_d goes down during a finite period of time. This situation is analogous to that when the circuitry that computes the desired voltage presents a fault during a time period. In an explicit form, the changes of the desired output voltage v_d are described in Table 5. The initial output voltage is $v(0) = 14$ [V]. For this set of experiments the saturation limits are $u_{\min} = 0.2$ and $u_{\max} = 0.8$. The PI controller is implemented using gains $k_P = 0.881$ and $k_I = 20$. The PIAW uses the same gains and $k_A = 5$. The supply voltage

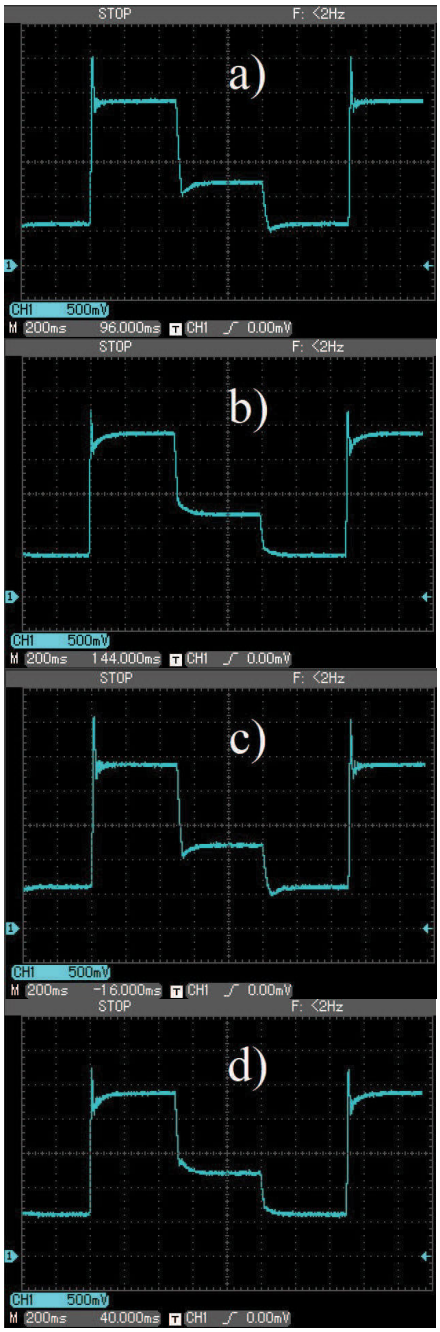

FIGURE 7. Experiment 4: Oscilloscope portraits when comparing with respect to pulse width modulation. *a*) PI control plus $\Sigma-\Delta$. *b*) PIAW control plus $\Sigma-\Delta$. *c*) PI control plus PWM. *d*) PIAW control plus PWM.

E is kept constant at 20 V. The results corresponding to this experiments are approximated in Figure 6. For $0 \leq t < 0.5$ [s], the PI controller is not able to deal with the input saturation and it results in poor performance since a large settling is observed in contrast with the performance of the PIAW scheme. During the fault time range $0.5 \leq t < 1$ [s] where $v_d = 0$ [V] the control input is kept to the lower saturation limit for both schemes as expected. However, when the fault is removed, i.e., for the time range $1 \leq t \leq 1.5$ [s] and $v_d = 14$ [V], the output voltage $v(t)$ reaches very fast the

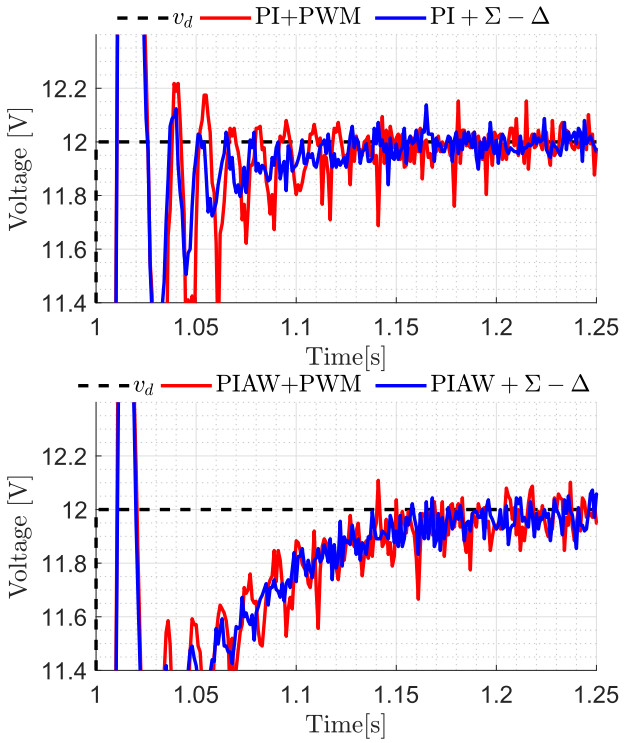

FIGURE 8. Experiment 4: Comparison in the implementation of the PI and PIAW controllers when using the Σ-Δ and the PWM technique.

desired value using the PIAW while $v(t)$ presents a very large settling time using the PI. The reason is that during the fault, the integrator of the PI scheme keeps accumulating a numerical value since the output voltage cannot reach the desired voltage due to the saturation. This is precisely a windup effect introduced by the limitation of the converter input. In contrast, the PIAW behaves very well even if saturation occurs.

F. EXPERIMENT 4: COMPARISON WITH RESPECT TO CLASSICAL PWM

In this set of experiments, the performance of the PI and PIAW schemes is tested by using different ways of enabling the gate of the MOSFET. In other words, four experiments have been carried out using the PI and PIAW controllers in combination with the Σ-Δ modulator in (29) and PWM technique. For the latter case study, the PWM module of the Delfino microcontroller was used at 12.5 kHz.

In particular, the conditions of Experiment 4 are the same as the ones used in Experiment 2. In other words, the supply voltage E is constant for all time, while the desired voltage v_d is changed in different time ranges as described in Table 3.

The differential probe DP10013 was used to measure the output voltage $v(t)$ with the oscilloscope UNI-T UTD4204C. The differential probe has a x50 attenuation factor and the oscilloscope has a x10 attenuation factor as a result each division in the vertical axis of the oscilloscope screen represents 2.5 [V].

The results are shown in Figure 7. For these experiments, oscilloscope portraits are given. It should be noticed from Figure 7 that at first sight no important differences are noticed in the settling time and percentage overshoot when using the PI either with $\Sigma-\Delta$ modulation or PWM technique. The same observation is given for the PIAW scheme.

In order to detect more details in the performance, the experimental data have been collected and shown in Figure 8 for the time range $1 \leq t \leq 1.25$ [s], where $v_d = 12$ [V]. Figure 8 shows that the output voltage is noisier when using the PWM technique than when implementing the $\Sigma-\Delta$ modulation. This evidence demonstrates that the $\Sigma-\Delta$ modulator is more suitable than the PWM in applications where a lower ripple and a smoother output voltage are required [15].

VI. CONCLUSION

In this work, the stabilization of the constantly perturbed DC-DC buck power converter was addressed by using an anti–windup PI approach. The controller design was divided into two steps. First, a PI-type controller to regulate the input-limited averaged buck power converter system was given. Second, the $\Sigma-\Delta$ modulation was used to transform the continuous input signal $u_{av}(t)$ into the set valued input $u_{sw}(t) \in \{0, 1\}$, which is used to enable the MOSFET gate. The main theoretical conclusion consisted in that the combination of the anti-windup PI controller and the $\Sigma-\Delta$ modulator assures globally stability of the state-space origin of the closed-loop system. To carry out the corresponding convergence analysis, Lyapunov's method was used. Although the DC-DC buck power converter presents input limitations into the range $(0, 1)$ the output voltage error goes asymptotically to zero for any initial conditions. To ensure the effectiveness of proposed control solution, a detailed real-time experimental study was achieved, having obtained convincing results. The experimental study confirmed the robustness of the PI with anti-windup control and the $\Sigma-\Delta$ modulation.

Further research consists in developing PI-type controllers equipped with integrator anti-windup and $\Sigma-\Delta$ modulation for more complex DC-DC power converters such as the boost, buck–boost and SEPIC power converters. Another interesting topic is the control of a DC-DC power converter driving an armature controlled DC motor tacking into account the limitation of the duty cycle percentage, such as has been done in this manuscript.

FINANCIAL DISCLOSURE

None reported.

CONFLICT OF INTEREST

The authors declare no potential conflict of interests.

APPENDIX

In this Appendix, the positiveness of expressions (7) and (8) is justified, and that $H(u)$ is radially unbounded. Please recall that $I = [\underline{u}, \overline{u}]$ and $I_0 = (\underline{u}, \overline{u})$.

To show the positiveness of the expression (7), assuming that $u > \overline{u}$, the following two subcases are analyzed: *i)* $u_s\overline{u} \geq 0$, and *ii)* $u_s\overline{u} < 0$.

Case (i) $u_s\overline{u} \geq 0$: since $u > \overline{u}$, the equation $u = \overline{u} + \eta$ is expressed, where $\eta > 0$. Consequently, equation (7) can be written as:

$$H(u) = \frac{1}{2}(\overline{u} - u_s)^2 + (\overline{u} - u_s)\eta + u_s\overline{u}.$$

The expression above allows us to conclude that $H(u) > 0$, because of $\overline{u} - u_s > 0$, according to (3), and $\eta > 0$. Besides:

$$\lim_{u\to\infty} H(u) = \lim_{\eta\to\infty} \frac{1}{2}(\overline{u} - u_s)^2 + (\overline{u} - u_s)\eta + u_s\overline{u} \to \infty.$$

Case (ii) $u_s\overline{u} < 0$: using once again that $u = \overline{u} + \eta$, with $\eta > 0$, equation (7) can be written as:

$$H(u) = \frac{1}{2}(\overline{u}^2 + u_s^2) + (\overline{u} - u_s)\eta - u_s\overline{u},$$

which is strictly positive definite since $\overline{u} - u_s > 0$. Similarly,

$$\lim_{u\to\infty} H(u) = \lim_{\eta\to\infty} \frac{1}{2}(\overline{u}^2 + u_s^2) + (\overline{u} - u_s)\eta - u_s\overline{u} \to \infty,$$

is shown. Following the same steps as before, $H(u) > 0$ if $u < \underline{u}$ is confirmed, and $H(u) \to \infty$ as long as $u \to -\infty$. Hence, $H(u)$ is radially unbounded and strictly positive definite for all $u \notin I_0$. Finally, u_s is a single minimum of $H(u)$.

REFERENCES

[1] T. K. Nizami, A. Chakravarty, and C. Mahanta, "Design and implementation of a neuro-adaptive backstepping controller for buck converter fed PMDC-motor," *Control Eng. Pract.*, vol. 58, pp. 78–87, Jan. 2017.
[2] S. Okada, T. Nunokawa, and T. Takeshita, "Digital control scheme of single-phase uninterruptible power supply," in *Proc. INTELEC-31st Int. Telecommun. Energy Conf.*, Oct. 2009, pp. 1–6.
[3] Y.-T. Lee, C.-S. Chiu, and C.-T. Shen, "Adaptive fuzzy terminal sliding mode control of DC-DC buck converters via PSoC," in *Proc. IEEE Int. Conf. Control Appl.*, Sep. 2010, pp. 1205–1209.
[4] C. S. Chiu, Y. T. Lee, and C. W. Yang, "Terminal sliding mode control of DC-DC buck converter," *Commun. Comput. Inf. Sci.*, vol. 65, pp. 79–86, Dec. 2009.
[5] T. Guo, S. Huang, and X. Wang, "Overcurrent protection control design for DC-DC buck converter with disturbances," *IEEE Access*, vol. 7, pp. 90825–90833, 2019.
[6] S. Shi, S. Xu, J. Gu, and H. Min, "Global high-order sliding mode controller design subject to mismatched terms: Application to buck converter," *IEEE Trans. Circuits Syst. I, Reg. Papers*, vol. 66, no. 12, pp. 4840–4849, Dec. 2019.
[7] P. H. Rani, S. Navasree, S. George, and S. Ashok, "Fuzzy logic supervisory controller for multi-input non-isolated DC to DC converter connected to DC grid," *Int. J. Electr. Power Energy Syst.*, vol. 112, pp. 49–60, Nov. 2019.
[8] M. Cucuzzella, R. Lazzari, Y. Kawano, K. C. Kosaraju, and J. Scherpen, "Voltage control of boost converters in dc microgrids with ZIP loads," 2019, *arXiv:1902.10273*. [Online]. Available: https://arxiv.org/abs/1902.10273
[9] S.-W. Seo and H. H. Choi, "Digital implementation of fractional order PID-type controller for boost DC–DC converter," *IEEE Access*, vol. 7, pp. 142652–142662, 2019.
[10] H. Sira-Ramírez, M. A. Aguilar-Orduña, and E. W. Zurita-Bustamante, "On the sliding mode control of MIMO nonlinear systems: An input-output approach," *Int. J. Robust Nonlinear Control*, vol. 29, no. 3, pp. 715–735, Feb. 2019.
[11] A. Soto, P. Alou, J. A. Oliver, J. A. Cobos, and J. Uceda, "Optimum control design of PWM-buck topologies to minimize output impedance," in *Proc. APEC. 17th Annu. IEEE Appl. Power Electron. Conf. Expo.*, vol. 1, Mar. 2002, pp. 426–432.
[12] X. Zhang, R. Min, B. Ji, D. Zhang, Y. Wang, and J. Li, "Voltage-extrapolative charge balance controller with charge compensation for flyback converter operating in DCM," *IET Power Electron.*, vol. 12, no. 11, pp. 2713–2721, Sep. 2019.
[13] A. El Aroudi, B. A. Martinez-Trevino, E. Vidal-Idiarte, and L. Martinez-Salamero, "Analysis of start-up response in a digitally controlled boost converter with constant power load and mitigation of inrush current problems," *IEEE Trans. Circuits Syst. I, Reg. Papers*, vol. 67, no. 4, pp. 1276–1285, Apr. 2020.
[14] O. Garcia-Alarcon and J. Moreno-Valenzuela, "Analysis and design of a controller for an input-saturated DC–DC buck power converter," *IEEE Access*, vol. 7, pp. 54261–54272, 2019.
[15] R. Silva-Ortigoza, F. Carrizosa-Corral, J. J. Gálvez-Gamboa, M. Marcelino-Aranda, D. Muñoz-Carrillo, and H. Taud, "Assessment of an average controller for a DC/DC converter via either a PWM or a sigma-delta-modulator," *Abstract Appl. Anal.*, vol. 2014, pp. 1–17, Jun. 2014.
[16] R. Silva-Ortigoza, V. M. Hernandez-Guzman, M. Antonio-Cruz, and D. Munoz-Carrillo, "DC/DC buck power converter as a smooth starter for a DC motor based on a hierarchical control," *IEEE Trans. Power Electron.*, vol. 30, no. 2, pp. 1076–1084, Feb. 2015.
[17] C. Olalla, R. Leyva, A. El Aroudi, and I. Queinnec, "Robust LQR control for PWM converters: An LMI approach," *IEEE Trans. Ind. Electron.*, vol. 56, no. 7, pp. 2548–2558, Jul. 2009.
[18] A. Benzaouia, H. M. Soliman, and A. Saleem, "Regional pole placement with saturated control for DC-DC buck converter through hardware-in-the-loop," *Trans. Inst. Meas. Control*, vol. 38, no. 9, pp. 1041–1052, Sep. 2016.
[19] A. E. Syed and A. Patra, "Saturation generated oscillations in voltage-mode digital control of DC–DC converters," *IEEE Trans. Power Electron.*, vol. 31, no. 6, pp. 4549–4564, Jun. 2016.
[20] A. Martinelli, P. Nahata, and G. Ferrari-Treate, "Voltage stabilization in MVDC microgrids using passivity-based nonlinear control," in *Proc. IEEE Conf. Decis. Control (CDC)*, Dec. 2018, pp. 7022–7027.
[21] S. Liu, F. Zhang, and W. Meng, "The soft start controller based on duty cycle presetting on low cost analogue devices," in *Proc. 8th Int. Conf. Power Energy Syst. (ICPES)*, Dec. 2018, pp. 130–134.
[22] M. Abdelmoula and B. Robert, "Bifurcations and chaos in a photovoltaic plant," *Int. J. Bifurcation Chaos*, vol. 29, no. 8, Jul. 2019, Art. no. 1950102.
[23] A. Iovine and F. Mazenc, "Bounded control for DC/DC converters: Application to renewable sources," in *Proc. IEEE Conf. Decis. Control (CDC)*, Dec. 2018, pp. 3415–3420.
[24] M. Malekzadeh, A. Khosravi, and M. Tavan, "An immersion and invariance based input voltage and resistive load observer for DC–DC boost converter," *Social Netw. Appl. Sci.*, vol. 2, no. 1, p. 78, Jan. 2020.
[25] M. Malekzadeh, A. Khosravi, and M. Tavan, "Observer based control scheme for DC-DC boost converter using sigma–delta modulator," *COMPEL-Int. J. Comput. Math. Electr. Electron. Eng.*, vol. 37, no. 2, pp. 784–798, Mar. 2018.
[26] B. K. Bose, *Modern Power Electronics and AC Drives*, vol. 123. Upper Saddle River, NJ, USA: Prentice-Hall, 2002.
[27] V. M. Hernández-Guzmán, R. Silva-Ortigoza, and D. Munoz-Carrillo, "Velocity control of a brushed DC-motor driven by a DC to DC buck power converter," *Int. J. Innov. Comput., Inf. Control*, vol. 11, no. 2, pp. 509–521, 2015.
[28] M. I. Angulo-Nunez and H. Sira-Ramirez, "Flatness in the passivity based control of DC-to-DC power converters," in *Proc. 37th IEEE Conf. Decis. Control*, vol. 4, Dec. 1998, pp. 4115–4120.
[29] H. Sira-Ramirez, R. Marquez, and M. Fliess, "Generalized PI sliding mode control of DC-to-DC power converters," *IFAC Proc. Volumes*, vol. 34, no. 13, pp. 699–704, Aug. 2001.
[30] A. Gensior, O. Woywode, J. Rudolph, and H. Guldner, "On differential flatness, trajectory planning, observers, and stabilization for DC–DC converters," *IEEE Trans. Circuits Syst. I, Reg. Papers*, vol. 53, no. 9, pp. 2000–2010, Sep. 2006.
[31] R. Silva-Ortigoza, J. R. García-Sánchez, J. M. Alba-Martínez, V. M. Hernández-Guzmán, M. Marcelino-Aranda, H. Taud, and R. Bautista-Quintero, "Two-stage control design of a buck converter/DC motor system without velocity measurements via Σ-Δ-modulator," *Math. Problems Eng.*, vol. 2013, pp. 1–11, Jun. 2013.
[32] R. Silva-Ortigoza, C. Márquez-Sánchez, F. Carrizosa-Corral, M. Antonio-Cruz, J. M. Alba-Martínez, and G. Saldaña-González, "Hierarchical velocity control based on differential flatness for a DC/DC buck converter-DC motor system," *Math. Problems Eng.*, vol. 2014, pp. 1–12, Apr. 2014.
[33] H. Sira-Ramírez, C. A. Nuñez, and N. Visairo, "Robust sigma–delta generalised proportional integral observer based control of a 'buck' converter with uncertain loads," *Int. J. Control*, vol. 83, no. 8, pp. 1631–1640, Aug. 2010.

[34] H. Sira-Ramírez and R. Silva-Ortigoza, "Sliding mode Σ-Δ modulation control of the boost converter," *Asian J. Control*, vol. 7, no. 4, pp. 349–355, Oct. 2008.
[35] H. Sira-Ramírez and V. F. Batlle, "Robust Σ–Δ modulation-based sliding mode observers for linear systems subject to time polynomial inputs," *Int. J. Syst. Sci.*, vol. 42, no. 4, pp. 621–631, Apr. 2011.
[36] H. Sira-Ramirez, R. Marquez-Contreras, and M. Fliess, "Sliding mode control of DC-to-DC power converters using integral reconstructors," *Int. J. Robust Nonlinear Control*, vol. 12, no. 13, pp. 1173–1186, 2002.
[37] H. J. Sira-Ramirez and R. Silva-Ortigoza, *Control Design Techniques in Power Electronics Devices*. London, U.K.: Springer-Verlag, 2006.
[38] J. K. Mann, S. Perinpanayagam, and I. Jennions, "Aging detection capability for switch-mode power converters," *IEEE Trans. Ind. Electron.*, vol. 63, no. 5, pp. 3216–3227, May 2016.
[39] J. Li, K. Pan, Q. Su, and X.-Q. Zhao, "Sensor fault detection and fault-tolerant control for buck converter via affine switched systems," *IEEE Access*, vol. 7, pp. 47124–47134, 2019.
[40] X.-H. Chang, J. Xiong, and J. H. Park, "Estimation for a class of parameter-controlled tunnel diode circuits," *IEEE Trans. Syst., Man, Cybern. Syst.*, vol. 50, no. 11, pp. 4697–4707, Nov. 2020.
[41] X.-H. Chang, J. Xiong, and J. H. Park, "Fuzzy robust dynamic output feedback control of nonlinear systems with linear fractional parametric uncertainties," *Appl. Math. Comput.*, vol. 291, pp. 213–225, Dec. 2016.
[42] A. Visioli, *Practical PID Control*. London, U.K.: Springer-Verlag, 2006.
[43] J. Moreno-Valenzuela, "A class of proportional-integral with anti-windup controllers for DC–DC buck power converters with saturating input," *IEEE Trans. Circuits Syst. II, Exp. Briefs*, vol. 67, no. 1, pp. 157–161, Jan. 2020.
[44] J. Guzman-Guemez and J. Moreno-Valenzuela, "Saturated control of boost DC-to-DC power converter" *Electron. Lett.*, vol. 49, no. 9, pp. 613–615, Apr. 2013.
[45] R. Schreier, G. C. Temes, and S. R. Norsworthy, Eds., *Delta-Sigma Data Converters: Theory, Design, and Simulation*. New York, NY, USA: IEEE, 1997.

CARLOS AGUILAR-IBANEZ was born in Tuxpan, Veracruz, Mexico. He graduated in physics from the Higher School of Physics and Mathematics, National Polytechnic Institute (IPN), Mexico City, in 1990. He received the M.S. degree in electrical engineering from the Research Center and Advanced Studies of the IPN (Cinvestav-IPN), in 1994, and the Ph.D. degree in automatic control, in 1999. Since 1999, he has been a Researcher with the Center of Computing Research of the IPN (CIC-IPN). As of 2000 he belongs to the National System of Researchers (SNI), Mexico. His research interests include nonlinear systems, system identification, observers, automatic control, and chaos theory.

JAVIER MORENO-VALENZUELA (Member, IEEE) received the Ph.D. degree in automatic control from the CICESE Research Center, Ensenada, Mexico, in 2002. From 2004 to 2005, he was a Postdoctoral Fellow with the Université de Liége, Belgium. He is currently with the Instituto Politécnico Nacional—CITEDI, Tijuana, Mexico. He is the author of many peer-reviewed journal and international conference papers. He authored the book entitled: *Motion Control of Underactuated Mechanical Systems* (Springer-Verlag, 2018). His research interests include nonlinear systems, mechatronics, and intelligent systems. He has served as a Reviewer of a number of prestigious scientific journals. He is currently an Associate Editor of the IEEE Latin America Transactions and *Mathematical Problems in Engineering*.

O. GARCÍA-ALARCÓN received the degree of engineer in electronic instrumentation from the Universidad Veracruzana—México, in 2002, and the Master of Science and Doctor of Science degrees in digital systems from the Instituto Politécnico Nacional—México, in 2013 and 2020, respectively. He is currently a Professor with CETYS Universidad-México and the ITS Cosamaloapan—México. His research interests include power electronics systems, robotics, renewable energy systems, automation, and instrumentation systems.

MIZRAIM MARTINEZ-LOPEZ received the B.S. degree in mechatronics engineering from the Instituto Tecnológico de Durango, in 2018. He is currently pursuing the M.Sc. degree with the Instituto Politécnico Nacional—CITEDI, Tijuana, Mexico. His current research interests include control of nonlinear systems, robotics, and power electronics.

JOSÉ ÁNGEL ACOSTA was born in Huelva, Spain. He received the Servo-Electrical and Mechanical Engineering degree from the University of Huelva, Spain, and the Electrical Engineering degree from the University of Seville, Spain, and the Ph.D. degree from the Automatic Control and Systems Engineering Department, University of Seville. He was a Marie Curie Control Training Site Fellow as a Member of the Centre National de la Recherche Scientifique (CNRS, France), Laboratoire des Signaux et Systèmes, Supélec, France, in 2003 and 2005. He joined that department as a Research Assistant, in 1999, where he is currently a Professor and a Research Member of the Automatic Control and Robotics Institute. Since 2005, he has also been a Visitor at the Laboratoire des Signaux & Systèmes, CNRS, France. He was an Academic Visitor researching with the Electrical & Electronic Engineering Department as a Member of the Control & Power Group, Imperial College London, U.K., in 2008, 2009, 2010, and 2011. His research interests include nonlinear control of dynamical systems with emphasis on electromechanical and robotic systems. He received the Ph.D. European Award, in 2005. He was nominated for the George S. Axelby Outstanding Paper Award in the IEEE Transactions on Automatic Control journal, in 2006.

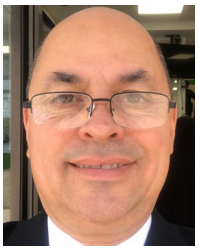

MIGUEL S. SUAREZ-CASTANON was born in Mexico, Mexico, in 1967. He received the B.S. degree in cybernetics and computer science from the School of Engineering, Lasalle University, in 1989, the M.S. degree in computer sciences from the Research Institute of Applied Mathematics and Systems, in 2001, and the Ph.D. degree in computer sciences from CIC-IPN, in 2005. Since 2007, he has been a member of the SNI of Mexico.